Supplementary Material

| Transcript	forward sequence 5'-3'	reverse sequence 5'-3	Reference
GAPDH	TGAAGCAGGCATCTGAGGG	CGAAGGTGGAAGAGTGGGAG	
TNFα	AGGCACTCCCCCAAAAGATG	GCTCCTCCACTTGGTGGTTT	
IL-1b	TGCCACCTTTTGACAGTGATG	AAGGTCCACGGGAAAGACAC	
CD44	GCACTGTGACTCATGGATCC	TTCTGGAATCTTGAGGTCTCC	(1)
TLR2	CCCTGTGCCACCATTTCC	CCACGCCCACATCATTCTC	(2)
MMP9	AAGGGGCGTGTCTGGAGATT	GGTACTGGAAGATGTCGTGTGAGT	(3)
MT1-MMP	GTGCCCTATGCCTACATCCG	CAGCCACCAAGAAGATGTCA	(2)
MMP2	CTGGAATGCCATCCCTGATAA	CAAACTTCACGCTCTTGAGACTTT	(3)
CCL2	TTTTGTCACCAAGCTCAAGAGA	ATTAAGGCATCACAGTCCGAGT	(4)
IL-6	TGAACAACGATGATGCACTTG	CTGAAGGACTCTGGCTTTGTC	

Supplementary Table 1. List of Primers used for qualitative Real-Time PCR.

A

mBECs

DAPI | CD31 | CD44 | Merge

CD44^fl/fl

Cd44^fl/fl x
VCad-Cre ER^T2

B

mBECs

DAPI | CD31 | CD44 | Merge

CD44^fl/fl

Cd44^fl/fl x
VCad-Cre ER^T2

C

Primary astrocytes

DAPI | GFAP | CD44 | Merge

CD44^fl/fl

Cd44^fl/fl x
GFAP-Cre

D

Primary microglia

CD11b | CD44 | Merge

CD44^fl/fl

Cd44^fl/fl x
Csf1R-Cre

BMD macrophages

DAPI | CD11b | CD44 | Merge

CD44^fl/fl

Cd44^fl/fl x
Csf1R-Cre

E

CD44 in GAMs

fold change to control

1.6
1.4
1.2
1.0
0.8
0.6
0.4
0.2
0.0

CD44^fl/fl

CD44^fl/fl x CSF1R Cre

****

Supplementary Figure 1. Conditional mouse lines validation.

(**A-B**) Validation of endothelial-specific CD44 depletion in CD44$^{fl/fl}$×Ve-Cadherin CreER^{T2} mice. Primary mouse brain endothelial cells (mBEC) were isolated from floxed controls and CD44$^{fl/fl}$×Ve-Cadherin CreER^{T2} mice and stained for CD44 (magenta), CD31(green), GFAP (cyan) and counterstained with DAPI (blue). Scale bars 50μm.(**A**) Representative images from CD44$^{fl/fl}$ and CD44$^{fl/fl}$×Ve-Cadherin CreER^{T2} mice. In mBECs from floxed mice, the majority of cells express CD44. In the CD44$^{fl/fl}$×Ve-Cadherin CreER^{T2} model, the number of CD44-positive cells is strongly reduced. (**B**) Representative images from CD44$^{fl/fl}$ and CD44$^{fl/fl}$×Ve-Cadherin CreER^{T2} mice showing the presence of CD44-positive contaminating astrocytes. In CD44$^{fl/fl}$ cultures, CD44 staining does not exclusively colocalize with GFAP staining. Conversely, in CD44$^{fl/fl}$×Ve-Cadherin CreER^{T2}, all CD44-positive cells are also positive for GFAP indicating those are astrocytes which tightly associate with endothelial cells. (**C**) Validation of astrocyte-specific CD44 depletion in CD44$^{fl/fl}$×GFAP-Cre mice. Mouse primary astrocytes were isolated from floxed controls and CD44$^{fl/fl}$×GFAP-Cre newborn mice, stained for GFAP (cyan) and CD44 (magenta) and counterstained with DAPI (blue). No CD44 staining was observed in CD44$^{fl/fl}$× GFAP-Cre cultures. Double-positive astrocytes were present only in CD44$^{fl/fl}$ controls. Scale bar 50μm. (**D**) Validation of myeloid-specific CD44 depletion in CD44$^{fl/fl}$×Csf1R-Cre mice. Upper panel: Mouse primary microglia were isolated from floxed controls and CD44$^{fl/fl}$×Csf1R-Cre newborn mice and stained for CD11b (green) and CD44 (magenta). Double-positive microglia were present in controls but not in CD44$^{fl/fl}$×Csf1R-Cre cultures. Lower panel: Bone-marrow derived (BDM) macrophages were isolated from floxed controls and CD44$^{fl/fl}$×Csf1R-Cre newborn mice, stained for CD11b (cyan), CD44 (magenta) and counterstained with DAPI (blue). Double-positive macrophages were present in controls but not in CD44$^{fl/fl}$×Csf1R-Cre cultures. Scale bars 50μm. (**E**) CD44 levels in GAMs isolated by MACS from tumor bearing floxed and CD44$^{fl/fl}$×Csf1R-Cre mice were evaluated by qRT-PCR. CD44 mRNA levels in CD44$^{fl/fl}$×Csf1R-Cre mice were 5-fold lower than in controls. Data are presented as mean ± SD. Student's t-Test, ****$p < 0.0001$.
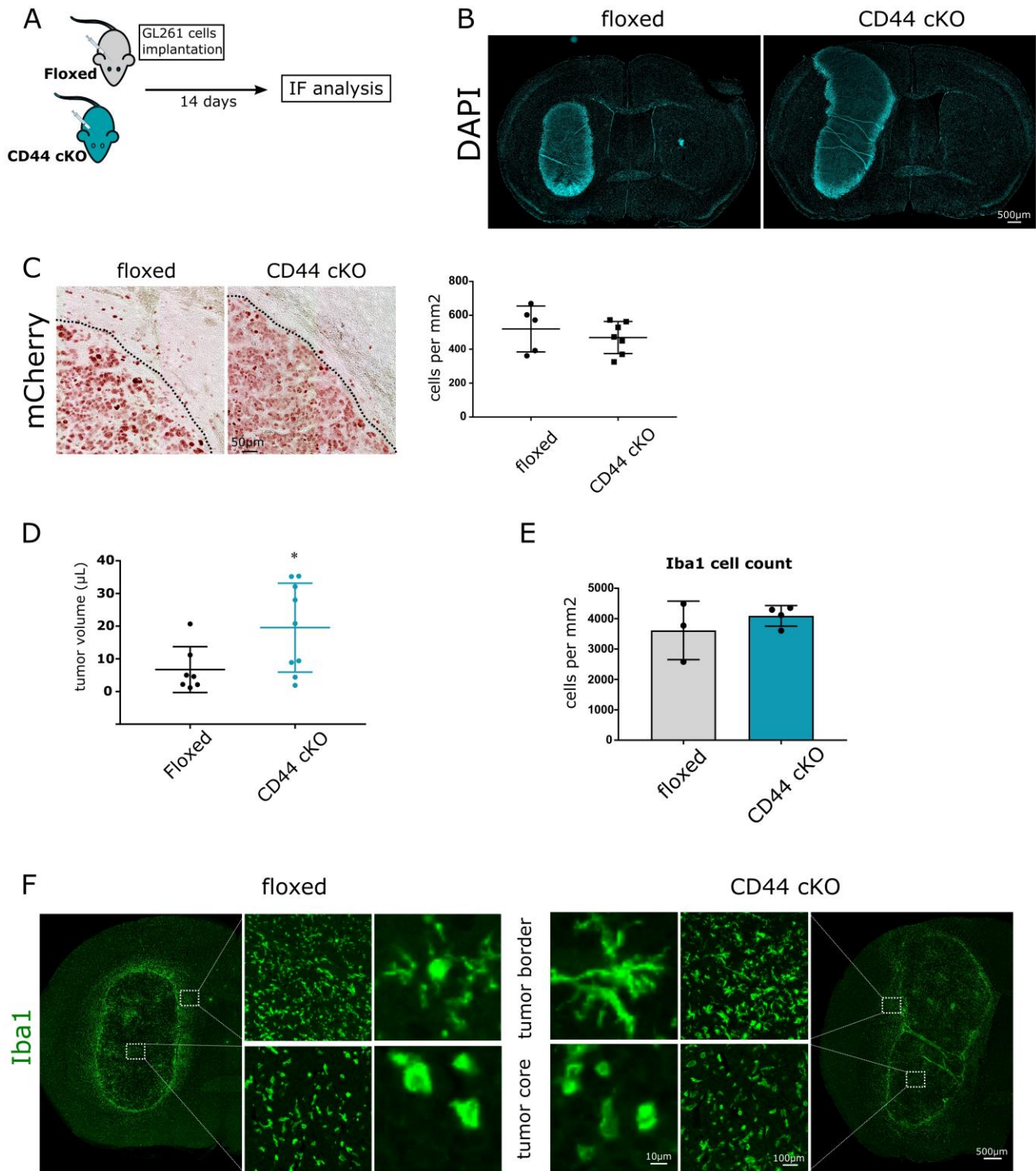
**Supplementary Figure 2.** Effects of Myeloid-specific CD44 knock-out on GL261 tumors in-vivo.

(**A**) 2×10^4 GL261 mCherry labelled cells were implanted in 5-8 weeks old floxed or cKO mice. Analysis were performed after 14 days. (**B**) Representative images of brains from floxed and cKO tumor-bearing mice stained with DAPI showing a bulk growth pattern. (**C**) Left-Representative images of tumors from floxed and cKO mice stained with mCherry. Dashed lines delimit the tumor

core. Right-Quantification of the number of mCherry-positive tumor cells migrating beyond the tumor border. The tumor border was manually drawn and the number of cancer mCherry-positive cells spreading in a radius of 300 microns was counted. (**D**) Tumor volume at 14 days, measured by MRI. Graph represent tumor volume (µl) for individual mice calculate from T2-weighted images. Data are presented as mean±SD. Student's t-Test, * $p < 0.05$. (**E-F**) Myeloid cells recruitment and morphology at endpoint. (**E**) Graphs depict the number of Iba1 positive cells per mm^2 in the tumor core. (**F**) Representative images of Iba1- positive cells. At the tumor border, labelled cells present with ramified morphology, whereas within the tumor core their morphology is amoeboid.
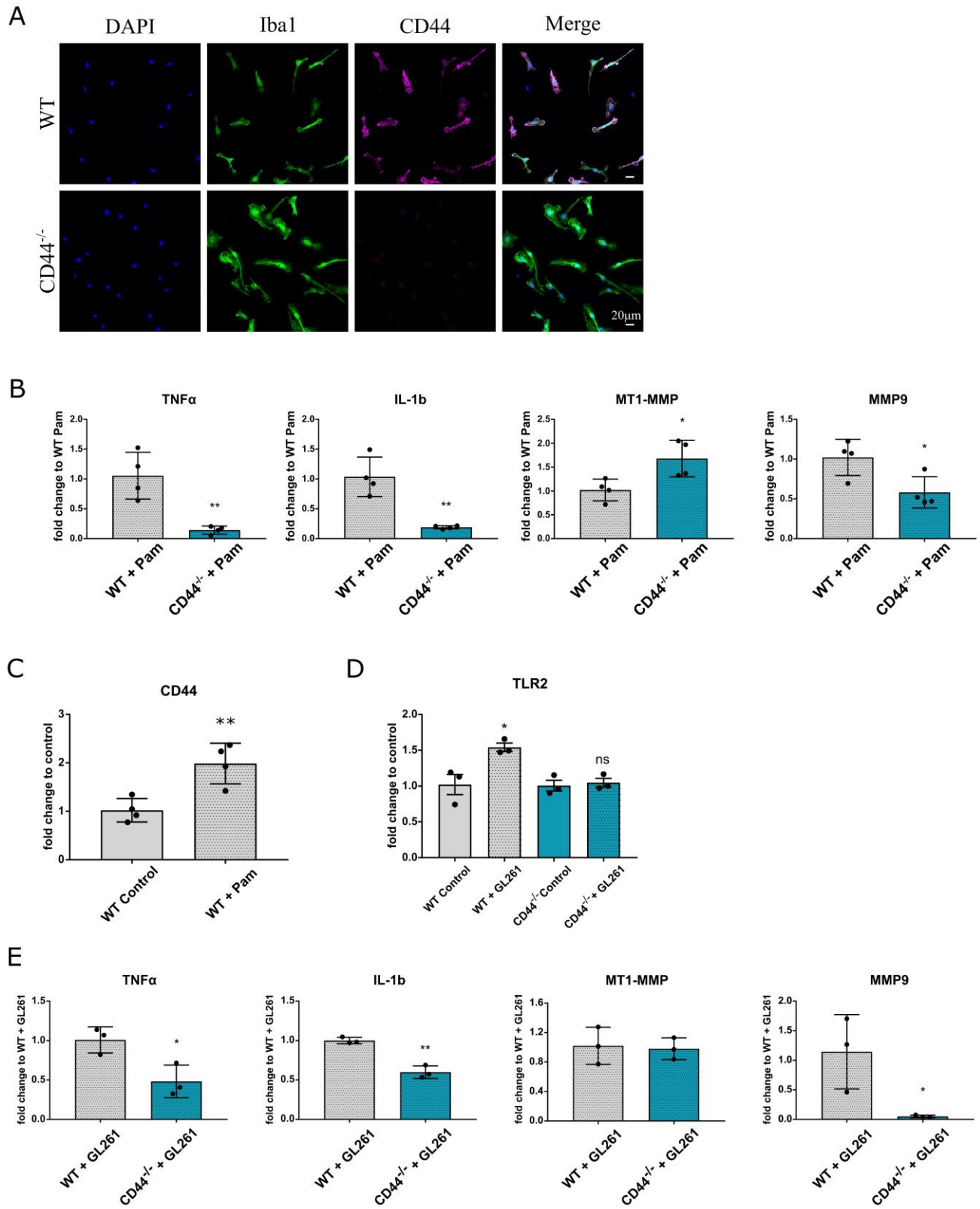
Supplementary Figure 3. CD44 and TLR2 signaling.

(**A**) Validation of the purity and CD44 expression in isolated primary microglia from WT and CD44$^{-/-}$ mice. Primary microglia were stained for Iba1 and CD44 and counterstained with DAPI. The representative image shows that all cells in the culture (DAPI) are positive for Iba1(green). Only cells isolated from WT mice co-express CD44 (magenta). (**B**) mRNA levels of TNF-α, IL-1b, MT1-MMP and MMP9 in primary WT or CD44$^{-/-}$ microglia after 6 hours of stimulation with the TLR2 agonist Pam3CSK4. Graph represents mRNA levels as fold change WT + Pam condition. Data are presented as mean±SD. Student's t-Test, * $p < 0.05$, ** $p < 0.01$. (**C**) mRNA levels of CD44 in primary microglia after 6 hours of stimulation with the TLR2 agonist Pam3CSK4. Graph represents mRNA levels as fold change to unstimulated control. Data are presented as mean±SD. Student's t-Test, ** $p < 0.01$. (**D**) mRNA levels of TLR2 in primary WT or CD44$^{-/-}$ microglia, after 24 hours co-culture with GL261 cells or "no cells" control condition. Graph represents mRNA levels as fold change to corresponding control. Data are presented as mean±SD. Student's t-Test, * $p < 0.05$ vs control, ns = not significant. (**E**) mRNA levels of TNF-α, IL-1b, MT1-MMP and MMP9 in primary WT or CD44$^{-/-}$ microglia after 24 hours co-culture with GL261 cells. Graph represents mRNA levels as fold change WT + GL261 condition. Data are presented as mean±SD. Student's t-Test, * $p < 0.05$, ** $p < 0.01$.
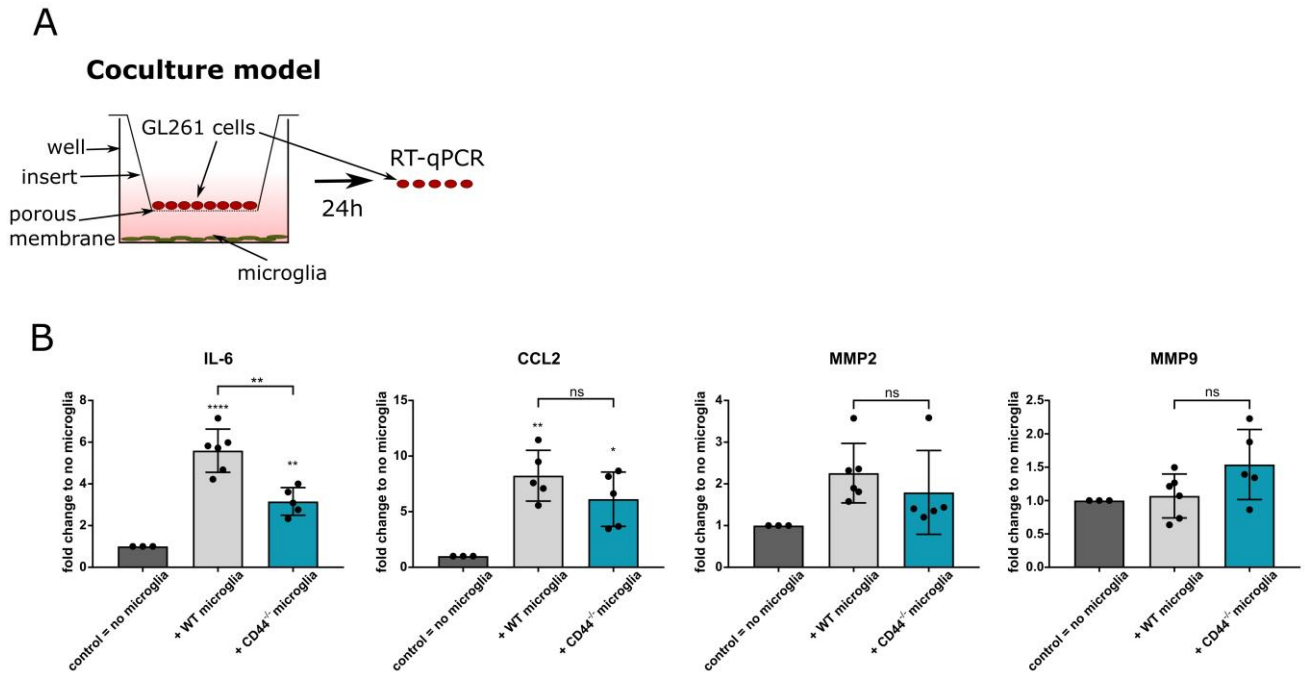
Supplementary Figure 4. qRT-PCR on GL261 cells co-cultured with WT or CD44$^{-/-}$ microglia.

(**A**) Schematic representation of the co-culture experiment. GL261 cells were co-cultured for 24 hours with primary microglia isolated from WT or CD44$^{-/-}$ mice. Total RNA from GL261 cells was extracted and processed for qRT-PCR analysis. GL261 cells cultured without microglia in the bottom compartment were used as control. (**B**) mRNA levels of IL-6, CCL2, MMP2 and MMP9 as fold change to culture without microglia. Data are presented as mean±SD. Student's t-Test, **$p < 0.01$, ****$p < 0.001$, ns = not significant.
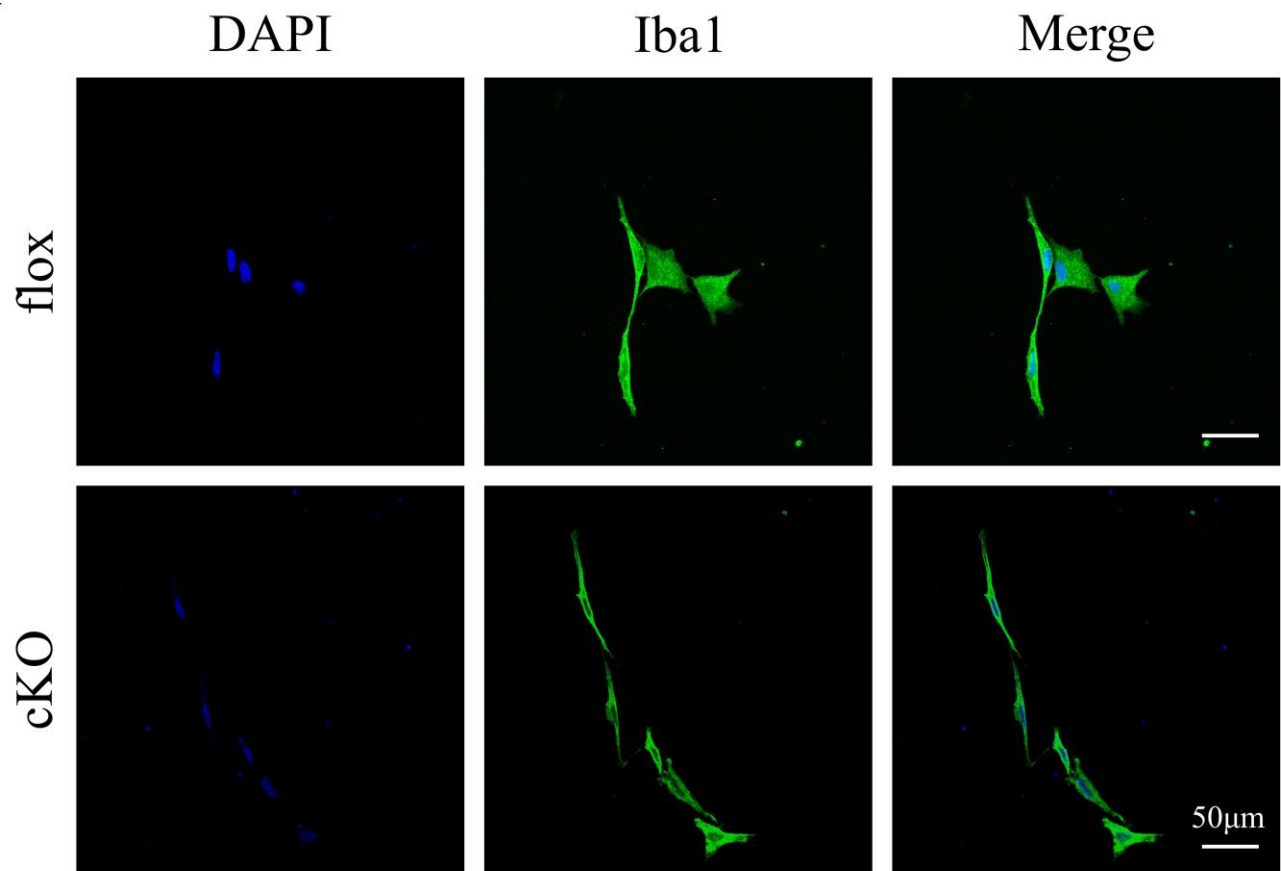
Supplementary Figure 5. Evaluation of the purity of cells isolated by MACS. 2×10^4 GL261 cells were implanted in 5-8 weeks old floxed or CD44 cKO mice and myeloid cells from tumor-bearing brains were isolated by MACS with Cd11b microbeads. Isolated cells were stained for Iba1 (green) and counterstained with DAPI (blue). The representative image shows that all purified cells (DAPI) are positive for Iba1.

References

1. Shatirishvili M, Burk AS, Franz CM, Pace G, Kastilan T, Breuhahn K, Hinterseer E, Dierich A, Bakiri L, Wagner EF, et al. Epidermal-specific deletion of CD44 reveals a function in keratinocytes in response to mechanical stress. *Cell Death Dis* (2016) 7: doi: 10.1038/CDDIS.2016.342

2. Vinnakota K, Hu F, Ku MC, Georgieva PB, Szulzewsky F, Pohlmann A, Waiczies S, Waiczies H, Niendorf T, Lehnardt S, et al. Toll-like receptor 2 mediates microglia/brain macrophage MT1-MMP expression and glioma expansion. *Neuro Oncol* (2013) 15:1457–1468. doi: 10.1093/NEUONC/NOT115

3. Del Zoppo GJ, Frankowski H, Gu YH, Osada T, Kanazawa M, Milner R, Wang X, Hosomi N, Mabuchi T, Koziol JA. Microglial cell activation is a source of metalloproteinase generation during hemorrhagic transformation. *J Cereb Blood Flow Metab* (2012) 32:919. doi: 10.1038/JCBFM.2012.11

4. Arendt LM, McCready J, Keller PJ, Baker DD, Naber SP, Seewaldt V, Kuperwasser C. Obesity promotes breast cancer by CCL2-mediated macrophage recruitment and angiogenesis. *Cancer Res* (2013) 73:6080–6093. doi: 10.1158/0008-5472.CAN-13-0926